Molecular Electronics

International Edition: DOI: 10.1002/anie.201605622
German Edition: DOI: 10.1002/ange.201605622

Molecular Conductance through a Quadruple-Hydrogen-Bond-Bridged Supramolecular Junction

Lin Wang[+], Zhong-Liang Gong[+], Shu-Ying Li, Wenjing Hong, Yu-Wu Zhong,* Dong Wang,* and Li-Jun Wan*

Abstract: *A series of self-complementary ureido pyrimidinedione (UPy) derivatives modified with different aurophilic anchoring groups were synthesized. Their electron transport properties through the quadruple hydrogen bonds in apolar solvent were probed employing the scanning tunneling microscopy break junction (STMBJ) technique. The molecule terminated with a thiol shows the optimal electron transport properties, with a statistical conductance value that approaches 10^{-3} G_0. The ^{1}H NMR spectra and control experiments verify the formation of quadruple hydrogen bonds, which can be effectively modulated by the polarity of the solvent environment. These findings provide a new design strategy for supramolecular circuit elements in molecular electronics.*

Understanding and controlling the electron transport process in a supramolecular assembly system associated through intermolecular interactions is an essential prerequisite for the fabrication of electronic circuits at the molecular level.[1] Apart from being efficiently synthesized in a user-friendly way, promising molecular assemblies for functional hybrid electronic devices should be structurally rigid and must facilitate electron transfer between individual components.[2] Various intermolecular forces have been explored in single-molecule electronics, including π–π stacking,[3] hydrogen bonding,[4] coordination bonds,[5] and charge transfer interactions.[6] Nevertheless, an ideal assembly scheme that satisfies all the aforementioned characteristics remains challenging.

Recently, multiple hydrogen bonds have been attracting great interest for constructing well-defined architectures in functional supramolecular polymers. Meijer et al.[7] utilized a self-complementary array with four cooperative hydrogen bonds associated by 2-ureido-4[1H]-pyrimidinone units in reversible self-assembling polymer systems. The high dimerization constant (10^5–10^7 M^{-1}) compensates for the limited strength of a single hydrogen bond.[7b,8] Moreover, the directionality and specificity of each hydrogen bond can maintain the beneficial planarity of a multiple-interaction-mediated complex during the dimerization,[9] which helps electronic devices maintain their conjugated structures after the self-assembly process. From the perspective of the synthesis, additionally, dimerization of even-numbered multiple hydrogen-bonding motifs can take place by homodimerization, bypassing the preparation of two different and yet complementary molecules.[10]

Herein, we investigate the electron transport properties of the modified self-complementary quadruple hydrogen-bonding UPy motifs with a definite assembled structure using the scanning tunneling microscopy break junction (STMBJ) method.[11] Three target UPy derivatives, **1**–**3**, were modified with different anchoring groups, thiol (SH), pyridyl (PY), and amino (NH_2), respectively (Figure 1a, synthetic details are summarized in the Supporting Information). A suitable single crystal for X-ray diffraction of **2** has been obtained by slowly diffusing petroleum ether into a 1,2-dichloroethane solution of **2**. Figure 1b,c shows that the two individual molecules of **2** are linked together by four hydrogen bonds (1.91 Å and 2.19 Å for C=O···H and N···H–N, respectively). At the same time, the formation of the intramolecular O···H–N hydrogen bond (1.87 Å) can help each monomer to keep a planar structure. These structural features result in the entire dimeric core of **2** occupying the same plane.

Homodimerization of the quadruple hydrogen-bonding motifs can be distinguished in the ^{1}H NMR spectra[10] and such self-assembled dimers are significantly affected by the polarity of the solvent. In the apolar solvent *o*-$C_6D_4Cl_2$, three singlet signals in the lower field (chemical shifts of 13.0, 11.6, and 10.6 ppm, Figure 2a) are clearly observed. These signals are attributed to the three different NH protons of a dimeric motif, in accordance with the literature.[12] However, when the protic solvent ethanol (C_2D_5OD) is introduced, the intensity as well as the position of these NH signals changes signifi-

[*] L. Wang,[+] S.-Y. Li, Prof. D. Wang, Prof. L.-J. Wan
Key Laboratory of Molecular Nanostructure and Nanotechnology, Institute of Chemistry, Chinese Academy of Sciences and Beijing National Laboratory for Molecular Sciences
Beijing 100190 (P.R. China)
E-mail: wangd@iccas.ac.cn

Dr. Z.-L. Gong,[+] Prof. Y.-W. Zhong
CAS Key Laboratory of Photochemistry, Institute of Chemistry, Chinese Academy of Sciences and Beijing National Laboratory for Molecular Sciences
Beijing 100190 (P.R. China)
E-mail: zhongyuwu@iccas.ac.cn

L. Wang,[+] Dr. Z.-L. Gong,[+] S.-Y. Li, Prof. Y.-W. Zhong, Prof. D. Wang, Prof. L.-J. Wan
University of the Chinese Academy of Sciences
Beijing 100049 (P.R. China)

L. Wang,[+] Prof. W. Hong
Department of Chemistry and Biochemistry, University of Bern
Freiestrasse 3, 3012 Bern (Switzerland)

Prof. W. Hong
Department of Chemical and Biochemical Engineering, College of Chemistry and Chemical Engineering, Xiamen University
Xiamen 361005 (P.R. China)
E-mail: whong@xmu.edu.cn

[+] These authors contributed equally to this work.

Supporting information for this article can be found under: http://dx.doi.org/10.1002/anie.201605622.

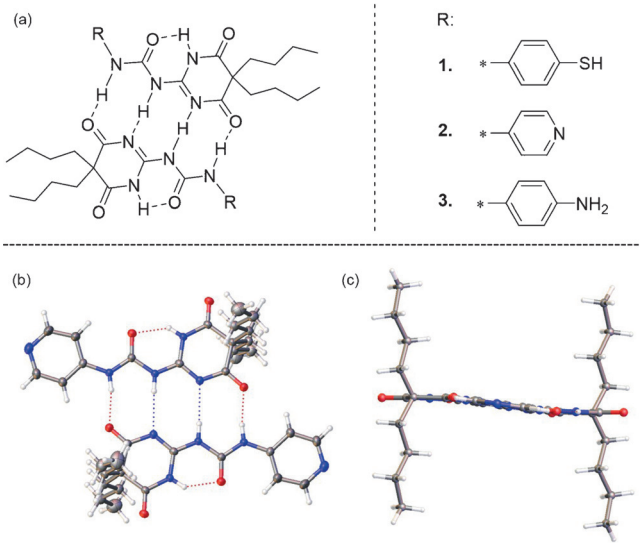

Figure 1. a) Molecular structures and self-assembly mode of Upy derivatives **1**–**3**. Single-crystal X-ray structure of dimeric **2** from the b) front and c) side view.[26]

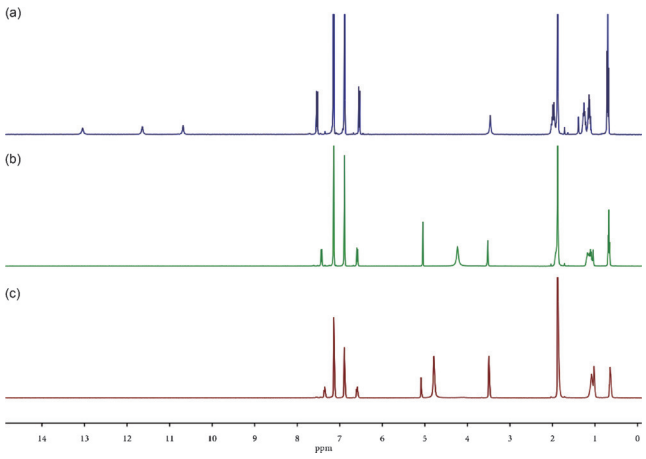

Figure 2. ^{1}H NMR spectra of compound **3** in different solvents: a) *o*-$C_6D_4Cl_2$, b) *o*-$C_6D_4Cl_2$/C_2D_5OD (4/1, v/v), and c) *o*-$C_6D_4Cl_2$/C_2D_5OD (2/1, v/v).

cantly. These low-field NH proton signals completely disappear when the volume ratio of [D_6]ethanol is 20% or more (Figure 2b,c), implying that the intermolecular hydrogen bonds have been largely disassembled. Similar solvent-dependent NMR spectral changes are also observed for the other two Upy derivatives **1** and **2**. It has been reported that two kinds of hydrogen-bonded dimer arrays, ADAD–DADA (A = acceptor, D = donor) dimers (minor) and AADD–DDAA dimers (major), can coexist in Meijer's 2-ureido-4[1*H*]-pyrimidinone motif, owing to the homodimerization of tautomeric monomers.[12,13] However, the ADAD tautomer and ADAD–DADA dimeric structure are effectively inhibited by the degenerate prototropy effect in the modified molecule.[14] This was supported by the ^{1}H NMR and X-ray diffraction data. Only the AADD–DDAA dimeric configuration was found in the crystallographic structure of **2** and one set of NH proton signal peaks was observed in the variable-temperature ^{1}H NMR experiments in *o*-$C_6D_4Cl_2$ (Supporting Information).

The electron transport characteristics of the single-molecule junctions formed by **1**–**3** were investigated in the apolar solvent 1,2-dichlorobenzene (DCB) using the STM break junction technique, as reported elsewhere.[11] Conductance-distance measurements were performed at a constant bias potential (V_{bias}) of 0.10 V between the tip and substrate. Tris(2-carboxyethyl)phosphine (TCEP) was employed in the molecular system of **1** to disrupt the disulfide bond.[15] Figure 3a shows typical semi-logarithmic conductance (G, in

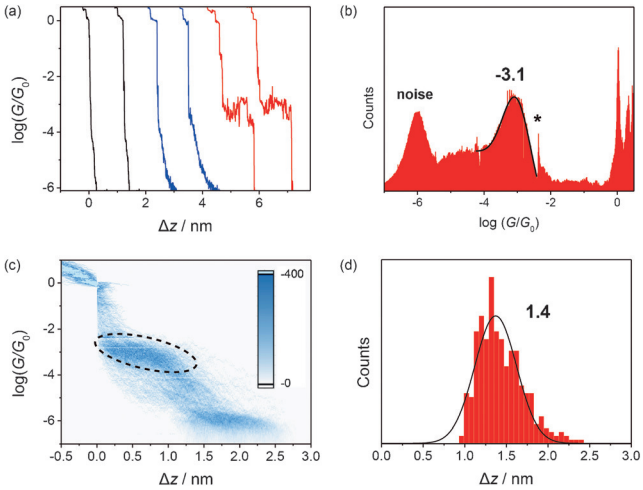

Figure 3. Single-molecule conductance results from STMBJ experiments at the indicated voltage of 0.10 V (tip positive). a) Typical conductance–distance curves (offset horizontally for clarity). b) 1D conductance histograms of **1** constructed from 347 conductance–distance curves that showed a pronounced plateau. c) 2D conductance histogram versus relative distance (Δz) of **1**. d) The stretching distance distribution of the molecular junction was obtained from the conductance region between $10^{-0.3}$ and $10^{-5.4}$ G_0. The asterisk (*) in the 1D histograms indicates an experimental artifact from the switching between different ranges in the linear amplifier of our STMBJ setup.

units of quantum point conductance $G_0 = 2e^2h^{-1}$) versus the relative electrode displacement (Δz) traces recorded for **1**. The presence of a plateau around G_0 corresponds to the formation of a single gold atom junction, which indicates atomically sharp electrodes. When there is no self-assembled dimeric molecule, the curve exhibits typical exponential decay after the tip has moved apart from the substrate (black curves). In the presence of 0.15 mM **1**, although most of the stretched curves show exponential decay (blue curves), certain individual curves exhibit pronounced plateaus (red curves), which suggests the formation a dimeric molecular wire of molecules of **1** bridged by the quadruple hydrogen bonds. To provide a quantitative insight into this process, thousands of stretching traces were recorded and only curves with clear plateaus were selected for the subsequent statistical analysis based on the criterion of stretching distance. The detailed selection method and all the data plots are described in the Supporting Information. The probability of the signal

curves is 14.7% for **1.** Figure 3b shows the one-dimensional (1D) conductance histogram, in which a well-defined conductance peak can be identified. Fitted to a Gaussian function, the prominent conductance peak with a most probable conductance value was centered at $10^{-3.1}$ G_0.

To obtain more information about the geometry of the junction, a two-dimensional (2D) histogram is shown in Figure 3c. We introduced a relative distance (Δz) and defined $\Delta z = 0$ at $10^{-0.3}$ G_0 to align all the stretching curves. Bright features, showing gold–gold contacts, are seen around $G = G_0$, followed by another well-defined conductance scatter group in the range of $10^{-2.5}$–$10^{-6.0}$ G_0. Calculations of the distances from the relative zero point to $10^{-5.4}$ G_0 yield the plateau length histogram (Figure 3d), which shows the junction stretching distribution. The electrode separation z_{exp} is then estimated by $z_{exp} = \Delta z + \Delta z_{corr}$, where $\Delta z_{corr} = 0.5 \pm 0.1$ nm corresponds to the quickly formed snap-back nanogap by the gold atoms.[16] The absolute displacement is $z_{exp} = 1.9 \pm 0.3$ nm. The distance between the two terminal S atoms of the dimer can be estimated to be about 18–19 Å from the crystal structure data of an analogue reported by Kikuchi's group.[17] The calibrated z_{exp} is comparable to the dimeric molecular length of **1**, which that the dimeric quadruple hydrogen-bonded derivative has been trapped between the gold electrodes.

Control experiments (Supporting Information) were also designed to verify the presence of the hydrogen bond conductance plateau. First, we performed the single-molecule conductance experiment in the DCB solution only with TCEP. As a result, the probability of selecting a molecular junction using our criterion decreased to 0.3%. This indicates that the conductance plateau stems from **1,** rather than the reductant or any contaminant in the environment. Moreover, when the protic solvent ethanol was introduced (volume ratio 4:1, for DCB and ethanol), 0.4% of the molecular junctions were detected as signal curves over thousands of stretching cycles. This phenomenon is in agreement with the disappearance of the low-field NH protons in the NMR experiments, which implies the disassociation of the quadruple hydrogen bonding self-assembly dimer. Additionally, the conductance was also measured at variable biases. In the low bias range from 0.05 to 0.15 V, we observed good reproducibility of the conductance. However, when the bias increased to 0.20 V, the conductance peaks became too shallow to identify, owing to the instability of the junction. All the experimental results discussed above demonstrate that the quadruple hydrogen-bond interaction is responsible for the observed electron transport of the tunneling junction.

Recently Lindsay et al. investigated a triple hydrogen-bonded assembly by STM combined with conducting atomic force microscopy (AFM) and determined conductance values between 10^{-6} and 10^{-5} G_0 for each molecular pair.[4a] Nishino et al. have characterized the electron transport between a pair of ω-carboxyl alkanethiols quantitatively and the conductivities of double hydrogen bonding are in the range of 10^{-5} to 10^{-4} G_0.[4b] The measured conductance value of the UPy thiol derivative in this work reached 10^{-3} G_0, which is significantly larger than those of the above-mentioned hydrogen-bonding systems. First, we note that the characterization methods are different. In these previous reports, the electrodes are functionalized with molecules prior to the conductance measurements, and the techniques for conductance measurement essentially evolve from the STM current-displacement [I(s)] method,[18] in which contact between tip and the substrate is avoided. This method has been shown more prone to detect only fully stretched configurations, which results in lower conductance values relative to the STMBJ method,[19] owing to the different junction formation process. Second, the structure of the investigated molecules has a significant influence on the conductance. Nishino et al. employed alkanethiols to construct the dimer molecular junction. Alkanes are relatively simple, but poorly conductive due to the large HOMO–LUMO gap. In the experiments conducted by Lindsay and coworkers, the deoxyribose ring connected with the anchoring thiol breaks the planar configuration, which may be unfavorable for the conductivity. In the molecules used herein, the four hydrogen bonds not only provide a strong connection between the monomers but also keep the entire core in the same plane, which has been shown experimentally to be advantageous for the conductance. The quadruple hydrogen-bonded dimer presents slightly higher or equivalent conductivity compared with other well-known conjugated molecular wires with comparable lengths, such as oligo(phenylene ethynylene) (OPE),[3b,11b,20] oligo(phenylene vinylene) (OPV)[21] and oligoyne.[22] This relative high conductance of quadruple hydrogen bonds may inspire further exploration for understanding the electron transport mechanism in the quadruple hydrogen-bonded system.

Single-molecule conductance was also measured with the quadruple hydrogen-bonded derivatives anchored by pyridyl (PY) and amino (NH_2) groups. Figure 4a,c show that most the probable values were fitted at $10^{-4.6}$ and $10^{-4.5}$ G_0 respectively, which are more than one order of magnitude lower compared with that of **1**. The lower conductance is mainly due to the weak electronic coupling between PY or NH_2 and the gold electrode.[16,23] Additionally, the junction formation probabil-

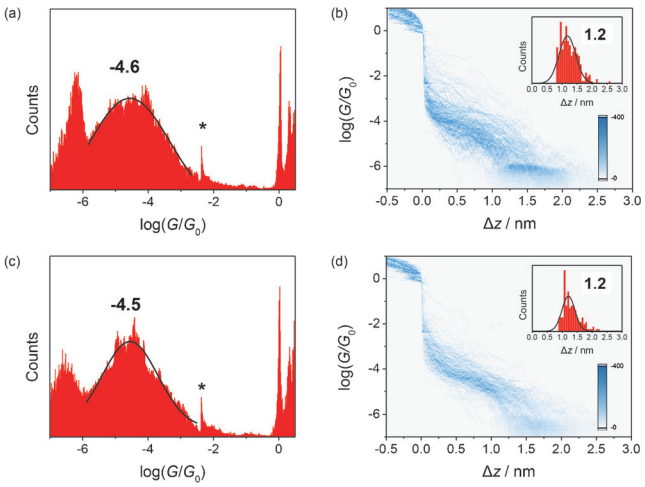

Figure 4. 1D and 2D histograms for compounds a),b) **2** and c),d) **3**. 259 out of 4907 and 147 out of 5687 curves showing distinguishable plateaus were selected to construct the histograms, respectively. Insets: Stretching distance distributions obtained between the conductance region $10^{-0.3}$–$10^{-5.4}$ G_0.

ities decreased to 5.2% and 2.6% for **2** and **3**, respectively, which indicates that it is more difficult for the PY- and NH_2-terminated derivatives to be trapped between the electrodes. The corrected absolute displacements obtained from the stretching distance histograms (insets in Figure 4b,d) are 1.7 ± 0.3 nm and 1.7 ± 0.2 nm, close to the lengths of **2** and **3**, which suggests that both PY and NH_2 are robust enough to hold the whole molecular junction firmly in place during the stretching process. Interestingly, both of the 1D histograms span from $10^{-3.0}$ to $10^{-6.0}$ G_0, which differs from the previous single-molecule junction measurements, in which PY and NH_2 linkages exhibit narrower distributions than SH.[16,24] The single molecular conductance results of **2** and **3** can be understood from the interplay between anchoring groups and the central molecular units. On one hand, previous studies found that rigid single-molecule junctions with PY and NH_2 linkages exhibit a well-defined conductance mainly owing to the uniform binding geometry.[16,24] The less complicated formation of a donor–acceptor bond between the N lone pair and gold atom requires the molecule to adopt a preferred orientation. However, for a supramolecular junction, the backbone of the quadruple hydrogen-bonded dimer has a comparatively vast bulk. The dangling of the molecule triggered by the thermal motion will hinder the emergence of the specific orientation, which leads to the significantly lower junction formation probability of the PY and NH_2 junctions. On the other hand, the donor–acceptor bond through the lone pair of an N atom shows a lower binding energy than a covalent Au–S bond.[25] It is noted that there are other N atoms in the backbone of UPy dimer besides those in the anchoring groups. These atoms can compete with the N atoms in anchoring groups and contribute to the formation of different configurations of the molecular junctions. The varied configurations lead to the large conductance variation of **2** and **3.** In the case of the SH anchoring group, **1** connects with the electrodes preferentially through the energetically favored Au–S covalent bond, compared with the coordinative bond between the gold and lone pair atoms. The molecular junction anchored by terminal SH groups dominates over the other configurations, leading to a more uniform conductance and higher junction formation probability. The overall results imply that the anchoring group has a significant influence on the conductance as well as the junction formation probability in the supramolecular assembled junction.

In conclusion, we have constructed quadruple-hydrogen-bond supramolecular junctions with ureido pyrimidinedione derivatives and investigated their electron transport characteristics using the STMBJ method. In comparison with the analogues of pyridine and amine, a molecular dimer with a thiol anchor displays the highest conductance value and largest junction formation probability. The most probable conductance approaches a magnitude of 10^{-3} G_0, which is comparable with that of fully-conjugated single molecular devices. This work suggests that a supramolecular assembly could also act as a highly conductive molecular electronics device, which offers a new design strategy and further extends the material library for future molecular electronic devices.

Acknowledgements

This work was supported by National Natural Science Foundation of China (21472196, 21433011, 21127901, 21233010, 21521062), and the Strategic Priority Research Program of the Chinese Academy of Sciences (Grant No. XDB12020100 and XDB12010400).

Keywords: electron transport · hydrogen bonds · molecular electronics · single-molecule junctions

How to cite: *Angew. Chem. Int. Ed.* **2016**, *55*, 12393–12397
Angew. Chem. **2016**, *128*, 12581–12585

[1] a) C. Joachim, J. K. Gimzewski, A. Aviram, *Nature* **2000**, *408*, 541–548; b) J. R. Heath, M. A. Ratner, *Phys. Today* **2003**, *56*, 43–49.

[2] E. D. Glowacki, M. Irimia-Vladu, S. Bauer, N. S. Sariciftci, *J. Mater. Chem. B* **2013**, *1*, 3742–3753.

[3] a) S. M. Wu, M. T. Gonzalez, R. Huber, S. Grunder, M. Mayor, C. Schonenberger, M. Calame, *Nat. Nanotechnol.* **2008**, *3*, 569–574; b) S. Martín, I. Grace, M. R. Bryce, C. Wang, R. Jitchati, A. S. Batsanov, S. J. Higgins, C. J. Lambert, R. J. Nichols, *J. Am. Chem. Soc.* **2010**, *132*, 9157–9164.

[4] a) S. Chang, J. He, A. Kibel, M. Lee, O. Sankey, P. Zhang, S. Lindsay, *Nat. Nanotechnol.* **2009**, *4*, 297–301; b) T. Nishino, N. Hayashi, P. T. Bui, *J. Am. Chem. Soc.* **2013**, *135*, 4592–4595.

[5] P. T. Bui, T. Nishino, *Phys. Chem. Chem. Phys.* **2014**, *16*, 5490–5494.

[6] P. T. Bui, T. Nishino, Y. Yamamoto, H. Shiigi, *J. Am. Chem. Soc.* **2013**, *135*, 5238–5241.

[7] a) R. P. Sijbesma, F. H. Beijer, L. Brunsveld, B. J. B. Folmer, J. H. K. K. Hirschberg, R. F. M. Lange, J. K. L. Lowe, E. W. Meijer, *Science* **1997**, *278*, 1601–1604; b) F. H. Beijer, H. Kooijman, A. L. Spek, R. P. Sijbesma, E. W. Meijer, *Angew. Chem. Int. Ed.* **1998**, *37*, 75–78; *Angew. Chem.* **1998**, *110*, 79–82.

[8] a) B. A. Blight, C. A. Hunter, D. A. Leigh, H. McNab, P. I. T. Thomson, *Nat. Chem.* **2011**, *3*, 244–248; b) T. Aida, E. W. Meijer, S. I. Stupp, *Science* **2012**, *335*, 813–817.

[9] Y. Yang, H. J. Yan, C. F. Chen, L. J. Wan, *Org. Lett.* **2007**, *9*, 4991–4994.

[10] C. Schmuck, W. Wienand, *Angew. Chem. Int. Ed.* **2001**, *40*, 4363–4369; *Angew. Chem.* **2001**, *113*, 4493–4499.

[11] a) B. Q. Xu, N. J. Tao, *Science* **2003**, *301*, 1221–1223; b) V. Kaliginedi, P. Moreno-García, H. Valkenier, W. J. Hong, V. M. García-Suárez, P. Buiter, J. L. H. Otten, J. C. Hummelen, C. J. Lambert, T. Wandlowski, *J. Am. Chem. Soc.* **2012**, *134*, 5262–5275.

[12] F. H. Beijer, R. P. Sijbesma, H. Kooijman, A. L. Spek, E. W. Meijer, *J. Am. Chem. Soc.* **1998**, *120*, 6761–6769.

[13] R. P. Sijbesma, E. W. Meijer, *Chem. Commun.* **2003**, 5–16.

[14] P. K. Baruah, R. Gonnade, U. D. Phalgune, G. J. Sanjayan, *J. Org. Chem.* **2005**, *70*, 6461–6467.

[15] J. A. Burns, J. C. Butler, J. Moran, G. M. Whitesides, *J. Org. Chem.* **1991**, *56*, 2648–2650.

[16] W. Hong, D. Z. Manrique, P. Moreno-García, M. Gulcur, A. Mishchenko, C. J. Lambert, M. R. Bryce, T. Wandlowski, *J. Am. Chem. Soc.* **2012**, *134*, 2292–2304.

[17] K. Tahara, T. Nakakita, S. Katao, J.-i. Kikuchi, *Chem. Commun.* **2014**, *50*, 15071–15074.

[18] W. Haiss, H. van Zalinge, S. J. Higgins, D. Bethell, H. Höbenreich, D. J. Schiffrin, R. J. Nichols, *J. Am. Chem. Soc.* **2003**, *125*, 15294–15295.

[19] W. Haiss, R. J. Nichols, H. van Zalinge, S. J. Higgins, D. Bethell, D. J. Schiffrin, *Phys. Chem. Chem. Phys.* **2004**, *6*, 4330–4337.

[20] a) Q. Lu, K. Liu, H. Zhang, Z. Du, X. Wang, F. Wang, *ACS Nano* **2009**, *3*, 3861 – 3868; b) Y. Xing, T.-H. Park, R. Venkatramani, S. Keinan, D. N. Beratan, M. J. Therien, E. Borguet, *J. Am. Chem. Soc.* **2010**, *132*, 7946 – 7956.

[21] R. Huber, M. T. González, S. Wu, M. Langer, S. Grunder, V. Horhoiu, M. Mayor, M. R. Bryce, C. Wang, R. Jitchati, C. Schönenberger, M. Calame, *J. Am. Chem. Soc.* **2008**, *130*, 1080 – 1084.

[22] a) P. Moreno-García, M. Gulcur, D. Z. Manrique, T. Pope, W. Hong, V. Kaliginedi, C. Huang, A. S. Batsanov, M. R. Bryce, C. Lambert, T. Wandlowski, *J. Am. Chem. Soc.* **2013**, *135*, 12228 – 12240; b) C. Wang, A. S. Batsanov, M. R. Bryce, S. Martín, R. J. Nichols, S. J. Higgins, V. C. M. García-Suárez, C. J. Lambert, *J. Am. Chem. Soc.* **2009**, *131*, 15647 – 15654.

[23] E. Leary, A. La Rosa, M. T. Gonzalez, G. Rubio-Bollinger, N. Agrait, N. Martin, *Chem. Soc. Rev.* **2015**, *44*, 920 – 942.

[24] a) J. Ulrich, D. Esrail, W. Pontius, L. Venkataraman, D. Millar, L. H. Doerrer, *J. Phys. Chem. B* **2006**, *110*, 2462 – 2466; b) L. Venkataraman, J. E. Klare, I. W. Tam, C. Nuckolls, M. S. Hybertsen, M. L. Steigerwald, *Nano Lett.* **2006**, *6*, 458 – 462.

[25] a) S. V. Aradhya, A. Nielsen, M. S. Hybertsen, L. Venkataraman, *ACS Nano* **2014**, *8*, 7522 – 7530; b) R. Frisenda, S. Tarkuc, E. Galan, M. L. Perrin, R. Eelkema, F. C. Grozema, H. S. J. van der Zant, *Beilstein J. Nanotechnol.* **2015**, *6*, 1558 – 1567.

[26] CCDC 1421013 contains the supplementary crystallographic data for this paper. These data are provided free of charge by The Cambridge Crystallographic Data Centre.

Received: June 11, 2016
Published online: August 31, 2016

